Activation of a Cl^- Current by Hypotonic Volume Increase in Human Endothelial Cells

BERND NILIUS, MASAHIRO OIKE, IVAN ZAHRADNIK, and GUY DROOGMANS

From the Department of Physiology, KU Leuven, Campus Gasthuisberg, B-3000 Leuven, Belgium

ABSTRACT We have used whole-cell and perforated patches to study ionic currents induced by hypotonic extracellular solutions (HTS, 185 mOsm instead of 290 mOsm) in endothelial cells from human umbilical veins. These currents activated within 30–50 s after application of HTS, reached a maximum value after ~50–150 s and recovered completely after re-exposing the cells to normal osmolarity. They slowly inactivated at potentials positive to +50 mV. The same current was also activated by breaking into endothelial cells with a hypertonic pipette solution (377 mOsm instead of 290 mOsm). The reversal potential of these volume-induced currents using different extracellular and intracellular Cl^- concentrations was always close to the Cl^--equilibrium potential. These currents are therefore mainly carried by Cl^-. DIDS only weakly blocked the current (K_I = 120 μM), while another Cl^--channel blocker, DCDPC (20 μM) was ineffective.

We were unable to record single channel activity in cell-attached patches but we always observed an increased current variance during HTS. From the mean current-variance relation of the whole-cell current records, we determined a single channel conductance of 1.1 pS. The size and kinetics of the current were not correlated with the concomitant changes in intracellular calcium. Furthermore, the currents could still be activated in the presence of 10 mmol/liter intracellular EGTA and are thus Ca^{2+} independent.

A similar current was also activated with iso-osmotic pipette solutions containing 300 μmol/liter GTPγS. Neomycin (1 mmol/liter), a blocker of PLC, did not prevent activation of this current. TPA (4 μmol/liter) was also ineffective in modulation of this current.

The HTS-induced current was completely blocked by 10 μmol/liter pBPB, a PLA_2 inhibitor. NDGA (4 μmol/liter) and indomethacin (5 μmol/liter), blockers of lipoxygenase and cyclo-oxygenase respectively, did however not affect the current induced by hypotonic solutions. The effects of arachidonic acid (10 μmol/liter) were variable. In 12 out of 40 cells it either directly activated a Cl^- current or potentiated the current activated by HTS. The membrane current was decreased at all potentials

Address correspondence to Guy Droogmans, Laboratorium voor Fysiologie, Campus Gasthuisberg, K.U. Leuven, B-3000 Leuven, Belgium.

J. GEN. PHYSIOL. © The Rockefeller University Press · 0022-1295/94/05/0787/19 $2.00
Volume 103 May 1994 787–805

in 18 cells, and was not affected in 10 cells. The HTS-induced currents may therefore be modulated by cleavage products of PLA_2, but not by messengers downstream of arachidonic acid.

Loading the cells with a segment of the heat stable protein kinase A inhibitor PKI (5–24) did not prevent activation of the HTS-induced current. It is therefore unlikely that HTS is signaled via a PKA-dependent pathway.

Verapamil (100 μmol/liter) and DDFSK (60 μmol/liter), both inhibitors of MDR1-gene encoded ATP-dependent ABC-transporters (P-glycoprotein), completely blocked the HTS-induced currents. HTS could still activate a current in the absence of ATP in the patch pipette. However, the rate of onset of the current became slower and its amplitude gradually declined during repeated exposure to HTS.

We propose that swelling of endothelial cells activates a chloride current, that may be related to P-glycoprotein. It is modulated via a G-protein-activated enzyme, but the nature of the second messenger is unknown. The PKC and PKA pathways are not involved in the regulation of the current.

INTRODUCTION

Swelling-activated K^+ and Cl^- currents, which may play a role in regulatory volume decrease, have been observed in many cell types, including epithelial cells, fibroblasts, chromaffin cells, tumor cells such as melanoma cells or HeLa cells (see for reviews Knoblauch, Montrose, and Murere, 1989; Grinstein and Foskett, 1990; McCarty and O'Neill, 1992; Nilius, 1993). The role of the cytoskeleton for activation of these channels is unclear, although dynamic changes in the cytoskeleton, especially in the actin filament organization (Sackin, 1989; Valverde, Diaz, Sepulveda, Gill, Hyde, and Higgins, 1992; Cantiello, Prat, Bonventre, Cunningham, Hartwig, and Ausiello, 1993), have been reported during cell swelling. Also the second messenger pathways that modulate these channels are not clearly understood.

Endothelial cells are continuously exposed to mechanical forces resulting from shear stress and stretch, that play an important role in the regulation of the biological activity of these cells (see for a review, Davies and Tripathi, 1993). The volume-activated effects reported in this study may therefore not only be of interest for evaluating the mechanisms of volume control, but may also provide some insight into the mechanisms by which endothelial cells respond to mechanical activation.

It has been reported that osmotic volume increase activates Ca^{2+}-dependent nonselective cation channels in endothelial cells (Ling and O'Neill, 1992). Also cyclic AMP has been shown to induce configurational changes in endothelial cells that are related to Cl^--efflux from the cells (Ueda, Lee, and Fanburg, 1990). We describe here that cell swelling induced by extracellular hypotonic solutions (HTS) activates a chloride current. This current is blocked by inhibitors of ATP-dependent ABC-transporters, P-glycoproteins, that are encoded by the multidrug-resistance gene (MDR1). Volume-activated currents in endothelial cells share some properties with those reported in chromaffin cells (Doroshenko, Penner, and Neher, 1991; Doroshenko, 1991; Doroshenko and Neher, 1992) and in T lymphocytes (Lewis, Ross, and Cahalan, 1993), but are essentially different from the large conductance, Ca^{2+}-

dependent Cl^--channels that have been described in endothelial cells (Groschner and Kukovetz, 1992; Olesen and Bundgaard, 1992; Vaca and Kunze, 1993).

An increased membrane conductance for Cl^- may not only reflect a possible role in volume regulation, but may also regulate the membrane resting potential of endothelial cells, and thereby stabilize the driving force for ionic fluxes, such as for Ca^{2+}.

MATERIALS AND METHODS

Isolation and Culture of Endothelial Cells

Endothelial cells were obtained from human umbilical cord veins by a collagenase digestion procedure, as described previously (Jaffe, Nachman, Becker, and Minick, 1973). Cells were grown in medium 199 containing 10% human serum, 2 mmol/liter L-glutamine, 100 U/ml penicillin and 100 μg/ml streptomycin. Cultures were maintained at 37°C in a fully humidified atmosphere of 10% CO_2 in air. The culture medium was exchanged every 48 h. Cells were detached by exposure to 0.05% trypsin in a Ca^{2+} and Mg^{2+} free solution for ~180 s and reseeded on gelatin coated coverslips. We kept the cells in culture 2–4 d before use. Under these conditions, cells were not confluent and single endothelial cells could be used for the experiments. We only used cells from primary culture to the second passage.

Current Measurements

Whole-cell membrane currents were measured using ruptured patches or patches perforated with nystatin to avoid disturbance of the intracellular Ca^{2+} buffering mechanisms (Horn and Marty, 1988). Currents were monitored with an EPC-7 (List Electronic, Darmstadt, Germany) or EPC-9 (Heka Electronics, Lambrecht Pfalz, Germany) patch clamp amplifier and sampled at an interval of 20 ms (2,048 points per record, filtered at 100 Hz). Single-channel activity was recorded in cell-attached patches (sampling interval 1 ms, 2,048 points per record, filter 200 Hz).

Current fluctuation analysis: mean current and variance were calculated from 100 ms current sweeps at −80 mV sampled at 10 kHz and collected at 1-s intervals before and during induction of the HTS-activated current. We also used for this purpose the currents recorded during the 100 ms voltage step to −80 mV in the voltage protocols shown in Fig. 1. These were sampled at 1 kHz and applied every 10 s. The HTS-induced current activates much slower than the sampling period of 100 ms, and can be considered as stationary during this period. Under these conditions, mean current I and current variance around the mean σ^2 are related by the expression (Sigworth, 1980)

$$\sigma^2 = i \cdot I - \frac{I^2}{N} \tag{1}$$

where i is the single channel current amplitude and N the total number of channels in the membrane. If the maximum open probability of the channel is low, the plot of σ^2 as a function of I will consist only of the rising limb of the parabola predicted by Eq. 1. It is under such conditions still possible to obtain a reliable estimate of i, but the estimation of N becomes uncertain. The single-channel chord conductance can be calculated from i and the electrochemical gradient, i.e., holding potential minus reversal potential of the HTS-induced current.

Solutions

The standard bath solution was a modified Krebs' solution of the following composition (in mmol/liter): 140 NaCl, 1.5 $CaCl_2$, 5.9 KCl, 1.2 $MgCl_2$, 11.5 HEPES-NaOH, 10 glucose, titrated

to pH 7.3 with NaOH. Osmolarity was 290 mOsm. "Low-Cl^-" bath solutions contained (mmol/liter): 70 Na_2SO_4, 2.8 KCl, 2 $CaCl_2$, 2 $MgCl_2$, 70 sorbitol, 11 HEPES (290 mOsm). Hypotonic solutions were obtained by diluting the normal Krebs solution with distilled water to 185 mOsm or by reduction of sorbitol from the low-Cl^- solution. Osmolarity of all the solutions was measured with a vapor pressure osmometer, Wescor 5500 (Schlag, Messinstrumente, Gladbach, Germany).

Except for cell-attached patches and for the whole-cell experiments in which we wanted to load some compound into the cell (GTPγS, neomycin, PKI, ATP, AA), the "perforated patch" technique was used (Horn and Marty, 1988, Korn and Horn, 1989). A nystatin stock solution of 50 mg/ml dissolved in DMSO was prepared and stored at −20°C. Immediately before use this stock solution was diluted 1,000 times to a final concentration of 50 μg/ml in the pipette solution and ultrasonicated. The tip of the pipette was filled with nystatin-free pipette solution by capillarity, and the pipette was then backfilled with nystatin-containing solution. Access occurred within 5–10 min. The pipette (internal) solution was made up in Milli-Q water (Millipore Corp., Bedford, MA) and contained (in mmol/liter): 100 K-aspartate, 40 KCl, 5 NaCl, 10 HEPES, 0.1 EGTA buffered at pH 7.2 with KOH, 290 mOsm/liter. Normal pipette solution for the perforated patch technique contained in addition 0.5 mmol/liter Na_2-ATP. For the experiments in which we studied the dependence of the current on the intracellular concentration of ATP, "ruptured" patches were used with patch pipette solutions containing either 0 or 4 mmol/liter Na_2-ATP (in the latter case no NaCl was added to the pipette). In Cl^--free pipette solutions, K-aspartate and KCl were replaced by 140 mmol/liter K-glutamate. Hypertonic pipette solutions were prepared by adding 50 mM mannitol to the normal pipette solution (osmolarity of 377 mOsm/liter). For single-channel experiments pipettes were filled with normal internal solution, the bath solution was the standard bath solution.

Experiments were performed at room temperature between 20 and 22°C. The following substances were used to modulate HTS-induced currents: DIDS (4,4′-diisothiocyanateostilbene-2,2′-disulphonic acid, Sigma), GTPγS (Sigma Chemical Co, St. Louis, MO), phorbol ester TPA (cells were pre-incubated for 10 min with 1 μmol/liter of the phorbol ester, 12-O-tetradecanoyl phorbol-13-acetate, Sigma Chemical Co.), NDGA (nordihydroguaiaretic acid, 4,4′-(2,3-dimethyl-1,4-butanedyl)-bis(1,2-benzenediol), dissolved in dimethyl sulphoxide [DMSO], Sigma Chemical Co.), neomycin (Sigma Chemical Co.), indomethacin (Indo, 1-[*p*-chlorobenzoyl]-5-methoxy-2-methylindole-3-acetic acid, Sigma Chemical Co.), DDFSK (1,9-dideoxyforskolin, Sigma Chemical Co.), DCDPC (3′,5′-dichlorodiphenylamine-2-carboxylic acid, Hoechst AG, Frankfurt, Germany), verapamil hydrochloride (Isoptine, Continental Pharma, Knoll), pBPB (4-bromophenacyl bromide, Sigma Chemical Co.) and arachidonic acid (Sigma Chemical Co.). Bath and pipette solutions with 10 μmol/liter arachidonic acid (AA) were stored after sonication in vials under pure N_2 at −20°C until use. AA was either added to the bath solution (35 cells) or loaded directly into the cells via the patch pipette (five cells). The results obtained with the latter procedure were similar to those obtained by bath application. To differentiate between a cAMP-mediated effect and a direct activation by HTS, we have done some experiments in which cells were loaded via the patch pipette with a peptide that specifically blocks the catalytic subunit of protein kinase A. This peptide consists of the amino acid residues 5–24 of the heat stable protein kinase A inhibitor (Knighton, Zheng, Ten Eyck, Xuong, Taylor, and Sowadski, 1991; PKI was kindly provided by Dr. M. Bollen, Department of Biochemistry, KU Leuven, Belgium). Pipette solution contained 2 μmol/liter PKI.

$[Ca^{2+}]_i$ Measurements

After loading with 2 μmol/liter fura-2/AM, cells on the cover slips were washed three times in the experimental chamber with Krebs' solution to remove extracellular fura-2/AM. Changes in intracellular Ca^{2+} were monitored by means of a photo multiplier-based system, consisting of

an inverted microscope (Zeiss IM 10), filter wheel, amplifier and controller (Luigs and Neumann, Ratingen, Germany) and a photo multiplier unit (Hamamatsu Corp., Toyooka Vill, Japan). The technique used was described in detail previously (Neher, 1989). In short, cells were illuminated alternatively at excitation wave lengths of 360 and 390 nm through a rotating filter wheel (speed between 2 and 3 revolutions/s). Excitation light was attenuated such that bleaching time constants exceeded more than 800 s. Auto fluorescence was measured on cell free parts of the cover slips and was automatically subtracted from the Ca^{2+} signals. Apparent concentration of free Ca^{2+} was calculated from the fluorescence ratio R (Grynkiewicz, Poenie, and Tsien, 1985):

$$[Ca^{2+}]_i = K_{eff}\frac{R - R_0}{R_1 - R} \tag{2}$$

where K_{eff} is the "effective binding constant," R_0 the fluorescence ratio at zero calcium and R_1 that at high Ca^{2+}. The calibration procedure was identical to that described previously (Schwarz, Callewaert, Droogmans, and Nilius, 1992). For data acquisition we used an eight channel A/D converter (Max Planck Institute for Biophysical Chemistry, Göttingen, Germany) connected to an ATARI Mega 4 system, which allowed simultaneous sampling of both fluorescence signals and transmembrane current.

Statistics

Pooled data are given by mean ± standard error of the mean. For significance, t test was used (level of significance, $p < 0.05$). Fitting routines were used from the software package FIG.P (Software Corp., Durham, NC).

RESULTS

Characterization of Ionic Currents Induced by Hypotonic Solutions (HTS)

Within 30 to 50 s after exposing endothelial cells to hypotonic extracellular solutions (HTS) a membrane current was activated that reached stationary values after 50 to 150 s. Relaxation of the current was rarely observed during maintained HTS. Fig. 1 depicts a typical experimental protocol to monitor this current: cells were clamped at a holding potential of 0 mV, every 10 s a voltage step to −80 mV with a duration of 0.8 s followed by a 5 s linear voltage ramp from −150 to +100 mV was applied. Fig. 1 *A* shows the voltage protocol and current traces recorded before application of HTS, at the maximum of the effect and after complete recovery. The current-voltage relationship reconstructed from these ramp protocols had a reversal potential of −17 mV which is close to the Cl^--equilibrium potential (−15.8 mV). The time course of the HTS-induced current was reconstructed from the mean current measured during the steps to −80 mV in consecutive records and is shown in Fig. 1 *B*. The arrows mark the times at which the records from *A* were taken. Changing back to isotonic solution induced in almost each experiment an overshoot of the current, which may be due to the higher Cl^--concentration in the iso-osmotic solution. The time course of the HTS-induced current was also measured during long lasting voltage steps of 150-s duration between −150 and +100 mV applied from a holding potential of 0 mV. A fast perfusion system was used to switch between hypotonic and iso-osmotic solutions. Fig. 1 *C* shows such a current trace during a voltage step to −120 mV. Exposure to hypotonic solutions for the time period indicated by the horizontal bar

induced an inward current which recovered after readmission of iso-osmotic solution, and turned into an outward current after stepping back to 0 mV. From 75 cells in which we simultaneously measured the membrane capacitance, we calculated a current density of 4.2 ± 0.22 pA/pF at −80 mV (capacitances ranged between 13 and 251 pF, current densities between 0.3 and 16.5 pA/pF).

Currents with a similar time course could also be activated in isotonic bath solutions by loading the cells with hypertonic pipette solutions in ruptured whole-cell mode. The current activated by this intervention also reversed close to the Cl^--equilibrium potential, and had a time course similar to that of the HTS-induced current (Fig. 1 *D*, same result in 4/4 cells). It is therefore likely that the HTS-induced currents are elicited by changes in osmolarity rather than by a reduction of ionic

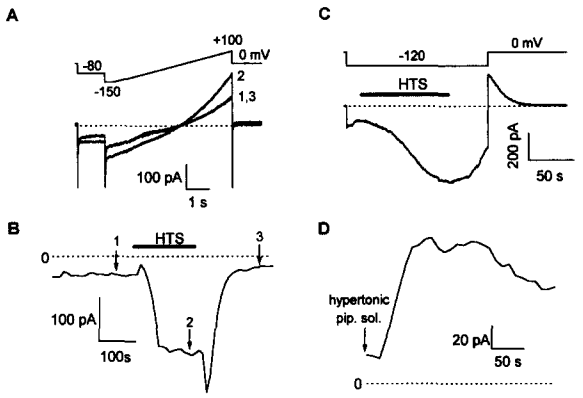

FIGURE 1. HTS-activated ionic currents in human endothelial cells. (*A*) Current traces, recorded during the voltage protocol shown in the top panel, before (*1*), at the maximum of the effect induced by HTS (*2*, 185 instead of 299 mOsm/liter), and after reperfusion with iso-osmotic solutions (*3*). The time at which these traces were recorded is indicated by the arrows in *B*.

(*B*) Averaged current values during the initial voltage step to −80 mV as a function of the time at which the voltage protocol was applied. The voltage protocol, as shown in *A*, was repeated every 10 s. The numbered arrows correspond to the traces shown in *A*. Note the current overshoot by changing back to isoosmotic solution.

(*C*) Time course of the membrane current activated by HTS during a long lasting voltage step to −120 mV (holding potential 0 mV, sampling interval 20 ms). The cells were superfused with hypotonic solution during the time period indicated by the horizontal bar. During recovery from HTS, the cell was clamped back to 0 mV, inducing an outward tail current.

(*D*) Breaking into an endothelial cell with a hypertonic pipette solution (377 mOsm/liter) induced an outward current at 0 mV.

strength. Application of a positive pressure of ~15 cm H_2O to the patch pipette also activated a current (three cells).

The size of the HTS-induced current was dependent on the osmolarity of the bath solution and clearly showed saturation at low osmolarities. Activation of the current had a threshold at 262 mOsm/l and half maximal activation of the current occurred at 221 ± 7 mOsm/l (n = 4 cells).

The HTS-induced currents slowly but incompletely inactivated at potentials positive to +50 mV. This is illustrated in Fig. 2, which shows families of membrane currents recorded during 12-s steps to potentials between −140 and +100 mV (20-mV step increments) under control conditions and 1 min after switching to HTS.

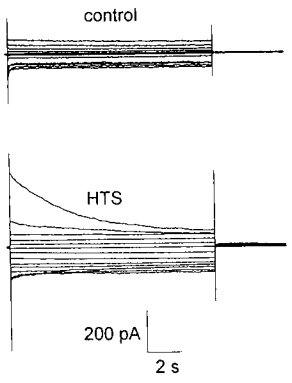

FIGURE 2. Voltage-dependence of the current induced by hypotonic solutions. Voltage steps from −140 to +100 mV (20-mV intervals) and 12-s duration were applied from a holding potential of 0 mV. Before exposure to hypotonic solutions, only small time-independent currents could be evoked (*top traces*). 60 s after exposure to hypotonic solution (*bottom traces*) larger currents could be recorded that slowly inactivate at large positive potentials.

The time constant of inactivation at +100 mV ranged between 2.7 and 37 s with a mean value of 10.7 ± 3.2 s (n = 7 cells).

The ionic nature of the current activated by hypotonic solutions was further studied in experiments, as shown in Fig. 3. Large outward currents could still be activated with 140 K-glutamate in the pipette instead of KCl, but inward currents were largely abolished. Fig. 3 *A* shows the time course of the current activated by HTS at different voltages. These traces were obtained from the mean current in a small voltage window in the ramp protocol around the potentials indicated along the traces. Almost no current was activated at −150 mV, but large outward currents were observed at +100 mV. The current-voltage relationships reconstructed from the voltage ramp protocols showed activation of outward currents by HTS, but virtually no inward currents (Fig. 3 *B*). The *I–V* curve of the HTS-induced current, obtained from the difference between the current traces during HTS and that under control conditions, showed no clear reversal potential, indicating that glutamate cannot be a charge carrier for this current.

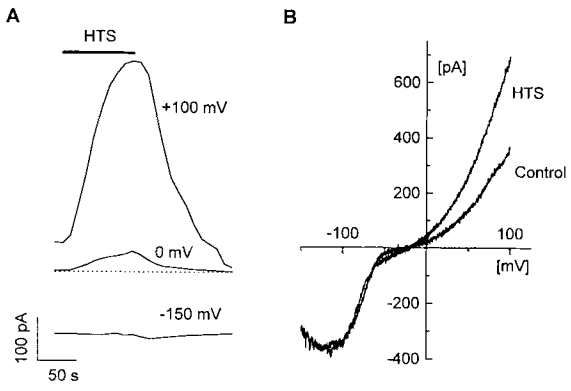

FIGURE 3. Ionic nature of the HTS-induced current. (*A*) Development and relaxation of the HTS-induced current at different voltages during ramp protocols, as shown in Fig. 1 *A*. The currents were calculated from a small window around the voltages indicated along the traces. Cl^- was substituted by glutamate in the pipette solution and no inward HTS-induced currents could be observed.

(*B*) Current-voltage relationships of the total membrane current of an endothelial cell before and during HTS in Cl^--free internal solution. Note again that virtually no inward current is activated by HTS at negative potentials.

Fig. 4 shows more directly the dependence of the HTS-induced current on the extracellular Cl^- concentration. Fig. 4 *A* shows the HTS activated current at a holding potential of +25 mV. Short application of a hypotonic low Cl^--solution induced a fast reduction of the outward current, that was immediately reversed after reapplication of the normal Cl^- solution. Fig. 4 *B* shows current-voltage relationships of the HTS-induced currents obtained from the same cell using ramp protocols (control currents were subtracted) in bath solutions with normal (90.8 mmol/liter) and reduced Cl^- (10.8 mmol/liter) concentration. The reversal potential was shifted

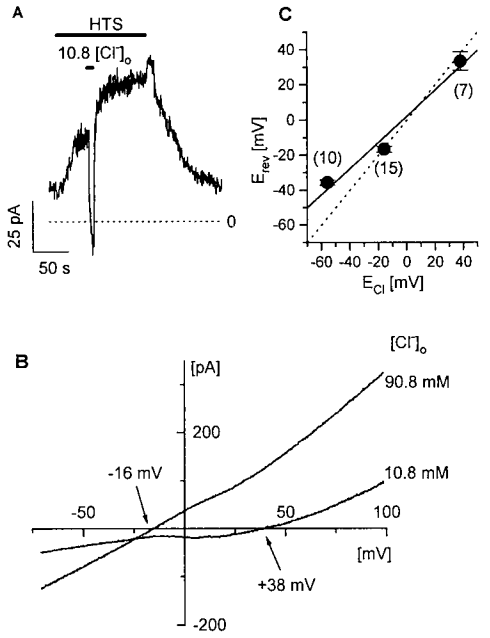

FIGURE 4. Activation of HTS-induced currents with Cl^- on either side of the membrane. (*A*) Outward current induced by HTS in an endothelial cell voltage-clamped at +25 mV. A short superfusion of the cell with 10.8 mmol/l Cl^- in the bath solution (E_{Cl} = +39.5 mV) largely abolished this outward current. This current was restored in normal Cl^--solution, and returned to its control level in isoosmotic solutions.

(*B*) Current-voltage relationships of the currents induced by hypotonic solutions (HTS) in 90.8 and in 10.8 mmol/l extracellular Cl^- ($[Cl^-]_o$). These curves, measured during voltage ramps from −80 to +100 mV, were obtained from the difference current during and before exposure to HTS. Reduction of extracellular Cl^- shifted the reversal potential to more positive values.

(*C*) Reversal potential (E_{rev}) of the HTS-induced current, obtained from difference currents as shown in *B*, as a function of the calculated Cl^- equilibrium potential (E_{Cl}). The number of cells for each data point is indicated along the symbol. The close correlation (r = 0.93) between both parameters, as shown by the full line, indicates that Cl^- is the main charge carrier of the HTS-induced current. The dotted line represents the expected relation for a purely Cl^--selective channel.

by 54 mV towards more positive potentials in the low Cl^- solution, which is close to the expected shift of 55.3 mV for a Cl^- selective conductance. Fig. 4 *C* shows the observed reversal potentials of the HTS induced current as a function of the corresponding Cl^--equilibrium potential. The close correlation between both potentials (r = 0.93, 32 cells) indicates that the HTS-activated current in endothelial cells is a Cl^- current.

Properties of the HTS-activated Conductance

We have tried to further characterize the nature of the HTS-induced change in a Cl^- conductance by using single-channel recordings and by analyzing the current fluctuations. In cell-attached patches (14 cells, holding potential = resting potential − 80 mV), we never observed channel activity during exposure to hypotonic solutions. However, the averaged current and its variance were reversibly increased during exposure to hypotonic solutions (not shown). Mean current (absolute values) and current variance were also calculated from whole-cell current recordings in isotonic solution and during exposure to HTS. Fig. 5 *A* shows the time course of the mean current and variance as calculated from the current recorded during the initial voltage step to −80 mV (see Fig. 1 *A* for protocol). Hypotonic solutions (as indicated by the horizontal bars) always enhanced the mean current (Fig. 5 *A*, *bottom*) and this was consistently accompanied by an increase of the current variance (Fig. 5 *A*, *top*).

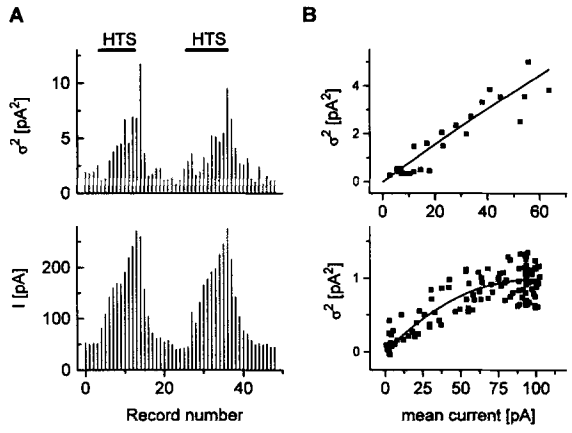

FIGURE 5. Increase in current fluctuations associated with HTS-induced currents. (*A*) Average current and current variance calculated from the initial voltage step to −80 mV (see Fig. 1 *A* for voltage protocol) in subsequent records in iso-osmotic and hypotonic solutions. HTS clearly increases the averaged current and its variance.

(*B*) Mean current-variance relation of whole-cell currents recorded during HTS at a holding potential of −80 mV. The continuous lines show the fit of the data to Eq. 1. Fitted parameters are i = 0.07 and 0.02 pA, N = 52,000 and 12,000 for the upper and lower panels, respectively.

Fig. 5 *B* shows two examples of the analysis of the mean current-variance relationship. The bottom shows an approximately parabolic relation without a descending limb, the top one does not reach a maximum value. The parabolic relation given by Eq. 1 was fitted to both data sets (*continuous line*) to obtain estimates of the single channel current amplitude i and the number of channels N. This procedure was applied to data obtained from 34 cells. From the current amplitude i and the reversal potential of the HTS-induced current obtained from the same cell, we calculated a unitary chord conductance γ = 1.1 ± 0.12 pS (n = 34 cells). The values for N were highly variable, which could be due to differences in cell surface area, but is most likely due to the absence of a plateau or a descending limb of the parabola in most plots of the variance versus mean current. Values for N ranged from 450 to 52,000 per cell, corresponding to maximum open probabilities p, calculated from the peak

macroscopic current I_{peak} by the equation $p = I_{peak}/N.i$, of 0.002 to 0.5. These values are rather similar to those reported by Lewis et al. (1993) for T-lymphocytes.

Effect of Cl^--Channel Blockers and Intracellular Calcium

The stilbene derivative DIDS inhibited the HTS-induced current in a concentration-dependent way. The block was however incomplete even at concentrations up to 200 μM. Fig. 6 *A* illustrates the rapid and reversible inhibition of the HTS-induced current during application of various concentrations of DIDS at a holding potential of −80 mV. The dose-response relationship of the current block is shown in Fig. 6 *B*, and shows, if we assume a complete inhibition at high DIDS concentrations, a half maximal inhibition at a concentration of 120 μM. DCDPC (20 μM), another compound that blocks Cl^--channels, did however not affect the HTS-induced current, but it suppressed the current in iso-osmotic solutions over the entire voltage

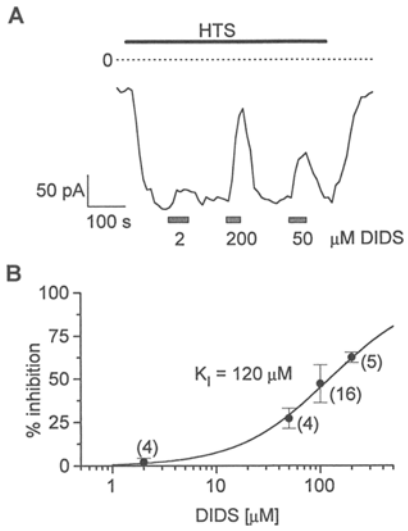

FIGURE 6. Block of HTS-induced current by DIDS. (*A*) HTS-induced current at −80 mV and its inhibition by various concentrations of DIDS. (*B*) Concentration response curve of the inhibition of the HTS-induced current by DIDS. The sigmoidal fit, assuming a complete inhibition at high DIDS concentrations, with a concentration of 120 μmol/liter for a half maximal inhibition is represented by the full line.

range. This rather low sensitivity, which was also observed at 0 mV, is consistent with the findings in T-lymphocytes (Lewis et al., 1993) where the degree of blockade is virtually absent at negative potentials but is more manifest at positive potentials.

To study the effect the intracellular Ca^{2+} concentration on the HTS-induced current, we have measured this current and $[Ca^{2+}]_i$ simultaneously. In 85% of the 59 cells that we studied, HTS induced an increase in $[Ca^{2+}]_i$ that was not correlated with the Cl^- current. This current could still be activated by HTS if the cells were loaded via the patch pipette with either 5 or 10 mmol/liter EGTA, but the rise in Ca^{2+} was abolished, as is shown in Fig. 7 *A*. In Fig. 7 *B* we have represented the maximal current activated by HTS as a function of $[Ca^{2+}]_i$ measured at the time of maximum current induction. These data were obtained from cells which were not loaded with EGTA. Both signals are obviously not correlated, indicating that the HTS-induced currents in human umbilical endothelial cells are independent of $[Ca^{2+}]_i$.

Modulation of HTS-induced Current by G-Proteins

It has been shown (Doroshenko et al., 1991) that loading of chromaffin cells with GTPγS activates a Cl^--current, which is identical to the volume-activated current. We have therefore tried to activate a current similar to the HTS-induced current by breaking into the cells with 300 μmol/liter GTPγS in the pipette. Fig. 8 *A* shows an experiment in which voltage ramps were applied every 10 s after breaking into the cell. Within 100 s after breaking into the cell, a current was induced (trace labeled GTPγS) that never occurred in normal whole-cell experiments in the absence of GTPγS. This current reversed near −12 mV and is apparently a Cl^--current (E_{Cl} = −15.6 mV).

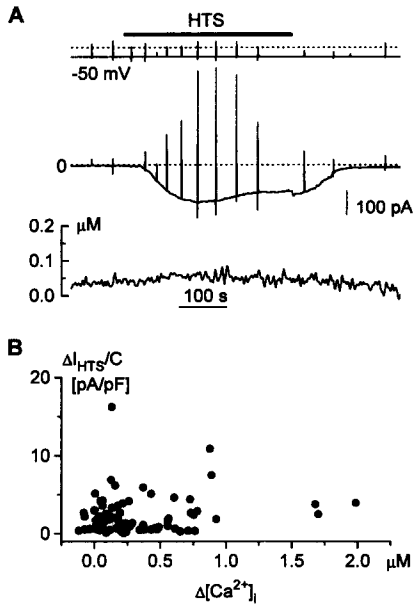

FIGURE 7. HTS-induced current is independent of the intracellular calcium concentration. (*A*) Membrane currents and intracellular calcium in a cell clamped at −40 mV before and during application of HTS. The cell was perfused with a pipette solution with 5 mmol/liter EGTA to buffer the increase in $[Ca^{2+}]_i$ which is normally observed during exposure to HTS. HTS activated a current in the absence of any increase in $[Ca^{2+}]_i$. Its reversal potential, determined from voltage ramps which appear as fast blips in the current trace, was −16 mV. The upper trace shows the clamped membrane potentials, the middle trace the membrane current, the lower one the changes in $[Ca^{2+}]_i$. (*B*) Amplitude of the HTS-induced current density measured at −80 mV as a function of the concomitant maximal rise in intracellular calcium (59 cells, nystatin perforated patches). It is apparent that there is no correlation between $[Ca^{2+}]_i$ and current. HTS-induced current densities were obtained by subtracting the current in iso-osmotic solutions from the HTS-induced current, and dividing this net current by the membrane capacitance. Also note the substantial scattering of the amplitude of the activated currents.

The outward currents which were activated by GTPγS at a holding potential of 0 mV disappeared in Cl^--deficient extracellular solutions (Fig. 8 *B*). These results hint to a possible contribution of G-proteins to the activation of this current. In this respect, the volume-activated current in endothelial cells resembles that in chromaffin cells (Doroshenko, 1991, Doroshenko et al., 1991). In accordance with the findings of Doroshenko and Neher (1992) we also observed that internal application of 250 μmol/l GDPβS via the patch pipette in the presence of 4 mmol/liter ATP significantly reduced the rate of activation of the HTS-induced current. The time for half-maximal activation was increased from 48 ± 3 s (n = 23 cells) in control cells to

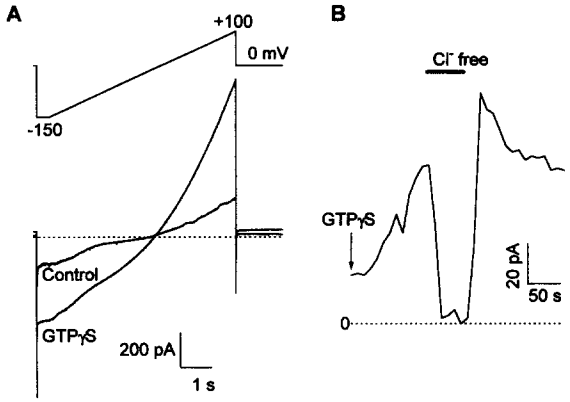

FIGURE 8. GTPγS activates a current that resembles the HTS-induced current. (*A*) Current traces recorded during repetitive application of the voltage protocol shown at the top after breaking into an endothelial cell with 300 μmol/liter GTPγS in the pipette. This procedure caused activation of a current that reversed at −12 mV (E_{Cl} = −15.8 mV).

(*B*) Time course of development of the GTPγS induced current measured at the 0 mV window at the end of the applied voltage protocols. The current disappeared in Cl^--free solutions.

91 ± 7 s (n = 6 cells) in the presence of GDPβS ($P < 0.01$). The amplitude of the HTS-activated current was however not significantly affected.

The Cl^--current activated by GTPγS could be indicative of a G-protein mediated activation. We have therefore checked putative targets of G-protein mediated actions. Neomycin (1 mmol/liter), a blocker of phospholipase C, which blocked the current in chromaffin cells, was without any effect in endothelial cells (six of six cells). Preincubation of the cells with an activator of protein kinase C, the phorbol ester TPA (2 μmol/liter), also did not affect activation of this current (six of six cells).

To quantify the degree of current activation by HTS and other compounds, the relative change in current ΔI_R was calculated from the current under control conditions I_{CONT}, and the current at the maximum of the effect, I_{EFF}, by

$$\Delta I_R = \frac{I_{EFF} - I_{CONT}}{I_{CONT}} \quad (3)$$

Fig. 9 summarizes the quantified experimental data for the various experimental conditions under which the Cl^- current was activated at 0 mV, but similar values were obtained at −80 and +100 mV.

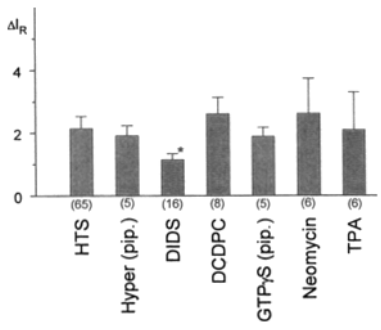

FIGURE 9. Synopsis of the activation of a Cl^- current by different interventions. Effects of various substances on the relative change in current ΔI_R induced by HTS. For comparison, we have also included the current induced by hypertonic pipette solution and by GTPγS. All effects were measured at 0 mV. The number of cells is indicated at the bottom of each bar. An asterisk marks the data which are significantly different from the control HTS-induced current.

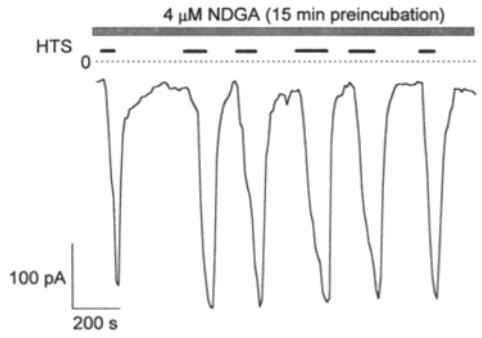

FIGURE 10. NDGA does not affect HTS-induced currents. In the presence of 4 μmol/liter NDGA, following a preincubation for 15 min with this compound, HTS was applied six times to the same cell. It is obvious that the amplitude of the current is not affected by NDGA. Note that HTS-induced currents can be repeated up to 30 times in the same cell without any significant change in amplitude or time course.

Effect of Arachidonic Acid and its Metabolites on the HTS-induced Current

Volume-activated currents in chromaffin cells (Doroshenko, 1991) could also be modulated by interference with PLA_2 upstream the cleavage of arachidonic acid. We have also assessed this pathway for endothelial cells. Application of 10 μmol/liter pBPB, a rather nonspecific inhibitor of PLA_2, completely and irreversibly blocked activation of the HTS-induced currents. This block developed slowly and was complete within ~20 min after application of pBPB. The same results were obtained in nine of nine cells.

The volume-activated current in chromaffin cells could also be modulated by interference with two pathways of the arachidonic acid metabolism. Block of the lipoxygenase with NDGA completely blocked the activation of the volume-dependent current in these cells. However, if applied to endothelial cells, NDGA (4 μmol/liter) did not affect activation of the HTS-induced current. Fig. 10 shows that after 15 min

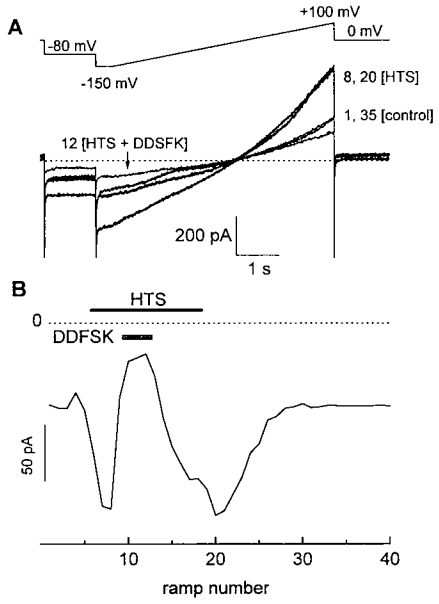

FIGURE 11. Block of HTS-induced current by DDFSK. (*A*) Current traces before (*1*), during (*8, 20*) and after application of HTS (*35*) (voltage protocol: *A*). DDFSK (60 μmol/liter) was applied during HTS (*12*). DDFSK completely and reversibly blocks the HTS-induced current.

(*B*) Time course of activation, block, unblock, and relaxation of the HTS-induced current obtained from the average current during the prepulse to −80 mV (*A*).

preincubation of the cells with NDGA the HTS-induced current could be activated without any change in amplitude during consecutive applications of HTS. It is therefore unlikely that a lipoxygenase pathway is involved in the regulation of this current. Also application of 4 μmol/liter indomethacin, a cyclo-oxygenase inhibitor, did not affect the HTS induced current (3 of three cells).

A possible explanation for the lack of any effects of NDGA and indomethacin and the block of the current with pBPB may be a direct action of arachidonic acid (AA). We have therefore tried to activate a Cl^- current by application of 10 μmol/liter AA. In only seven out of 40 cells a direct activation of a Cl^- current by AA was observed. In another five cells AA had no direct effect, but the HTS-induced current was increased in the presence of AA. In the remaining cells there was either no effect (10 cells) or even a decrease of the membrane current in the presence of AA (18 cells).

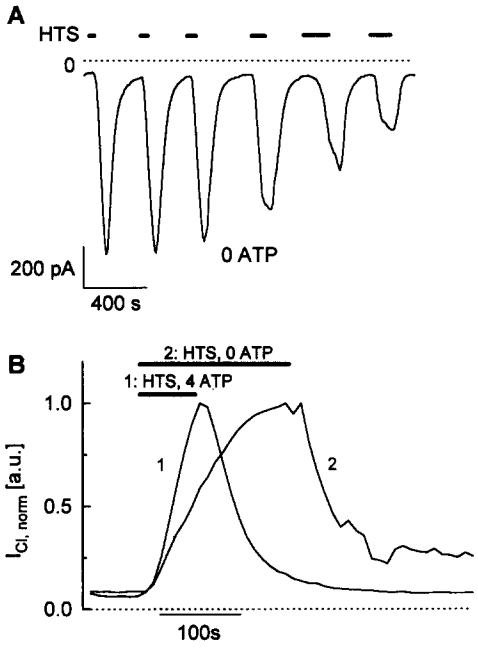

FIGURE 12. Effects of perfusion with ATP-free pipette solutions on HTS-induced currents. (*A*) HTS-induced currents measured in the ruptured whole cell configuration in the absence of ATP in the patch pipette. Currents were measured at the −80 mV pulses at the beginning of the voltage protocol, as shown in Fig. 1 *A*, which was applied every 10 s. The amplitude of the HTS-induced current gradually declined during subsequent applications of HTS.

(*B*) Scaled HTS-induced current traces after breaking into a cell with either 4 mmol/liter ATP (*1*) or with ATP-free pipette solution (*2*). It is obvious that activation of the HTS-induced current is slower in ATP-depleted cells.

Effect of Protein Kinase A Inhibitors on HTS-induced Currents

The involvement of the protein kinase A pathway in the activation of the HTS induced Cl^--current was assessed by loading the endothelial cells via the patch pipette with 2 μmol/liter of the protein kinase A inhibitor PKI, obtained from a segment of the heat stable protein kinase inhibitor (peptide residues 5 to 24, Knighton et al., 1991). Activation of the HTS-induced Cl^- current was not changed in these cells. It is therefore unlikely that the HTS-induced current is modulated by activation of PKA.

The HTS-induced Current May Be Induced by P-Glycoproteins

The most striking effects on HTS-induced currents were obtained by compounds that are known to inhibit ABC transporters (P-glycoprotein-mediated drug transport) and volume-regulated Cl^- channels in secretory epithelial cells and NIH3T3 fibroblasts transfected with the multidrug-resistance gene 1 (MDR1 gene, Valverde et al., 1992, Diaz, Valverde, Higgins, Rucareanu, and Sepulveda, 1993). Fig. 11 shows an example of the complete block of the HTS-induced current by application of DDFSK. Voltage ramp protocols, as shown in figure 11 *A* (*top*), were applied every 10 s. Exposure to hypotonic solution (starting from ramp 4) induced an increase in current (ramp 8). Application of 60 μmol/liter DDFSK caused a fast and complete inhibition of this current (ramp 12), which was completely restored after washing out DDFSK (ramp 20). Finally, superfusion of the cells with iso-osmotic solution restored the initial current-voltage relationship (ramp 35). Fig. 11 *B* shows the time course of activation and block of the HTS-induced current at −80 mV (mean current during the voltage

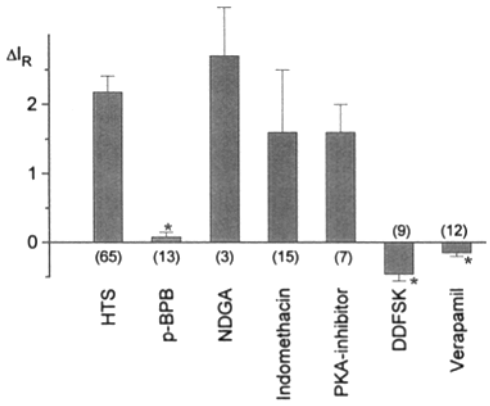

FIGURE 13. Synopsis of the modulation of the HTS-activated Cl^- current. The effects of various substances on HTS-induced currents are quantified by formula [3]. The number of cells are shown at the bottom of each bar. Data which are significantly different from control are indicated by an asterisk.

step). It is obvious that DDFSK completely and reversibly blocked the HTS-induced current. Verapamil (100 μM), another compound which is known to inhibit ABC-transporters, also completely and reversibly blocked the HTS-induced current.

These results suggest that P-glycoproteins are likely involved in the generation of the volume-induced current. Gill, Hyde, Higgins, Valverde, Minteng, and Sepulveda (1992) have shown that binding of ATP is sufficient to enable activation of the channel mode of the P-glycoprotein. Therefore, if the Cl^--channel would be a P-glycoprotein, depletion of intracellular ATP should diminish the HTS-induced current. We have therefore perfused the cell in the "ruptured" whole cell mode with ATP-free pipette solution. Under normal conditions, i.e., nystatin perforated patches or ruptured patches with ATP in the pipette solution, the HTS-induced current could be activated up to 30 times from the same cell. In the absence of ATP the HTS-induced current declined gradually during repetitive exposures to HTS, and its rate of activation became slower (Fig. 12). The latter became more obvious if the decreased currents were normalized to the size of the control, as shown in Fig. 12 *B*.

This effect of ATP-free solution was accelerated in the presence of 1 mmol/liter KCN and 2 mmol/liter 2-deoxyglucose in the bath. Similar results were obtained from 12 cells.

Fig. 13 summarizes the quantified data obtained from averaged currents during the voltage step to −80 mV for the various experimental protocols that we have used. Negative values indicate that the measured current was even decreased below the control current. The blockers of the ABC-transporter DDFSK and verapamil were highly effective inhibitors of the HTS-induced current. No significant changes in the activation of the HTS-induced current were obtained in the presence of NDGA, indomethacin, and PKI (intracellular). Inhibition of PLA_2 however induced a complete block of the HTS-induced current.

DISCUSSION

Volume-sensitive ion channels-permeable to K^+, Cl^- or nonselective cation channels have been described in various nonexcitable cells in which they play an important role for volume regulation (see Hoffmann and Simonson, 1989; Knoblauch et al., 1989; Morris, 1990; Nilius, 1993, for a review). Regulatory volume decrease in response to cell swelling has also been described in endothelial cells (Kempski, Spatz, Valet, and Baethman, 1985; O'Neill and Klein, 1992), but the mechanism is still unclear.

The results described in this report provide evidence for the activation of a chloride current by hypotonic solutions. Hypertonic solutions applied to the cytosol activate a similar current. It is therefore likely that these currents are activated by cell swelling due to applied osmotic gradients. HTS-activated currents reversed close to the expected Cl^- equilibrium potential, inward currents were almost completely abolished when intracellular Cl^- was substituted by glutamate and outward currents disappeared in the absence of extracellular Cl^- (Figs. 3 and 4). The current activated by HTS is therefore mainly carried by Cl^-.

It is intriguing to speculate that cell swelling interferes with the cytoskeleton and increases the open probability of ion channels in endothelial cells. Endothelial cells are able to sense changes in mechanical events like shear stress and stretch, but it is largely unknown how these physical forces modulate endothelial actions. In this respect, our results may be of interest as an example of a mechanically activated ion channel.

Our data, showing activation of a low conductance, Ca^{2+}-independent Cl channel, are at variance with those obtained from bovine aortic endothelial cells in which hypotonic solutions induced a 28-pS, Ca^{2+}-permeable nonselective cation channel (Ling and O'Neill, 1992). In this respect, the situation in our endothelial cells is more similar to that in chromaffin cell in which HTS induced a low conductance Cl^- channel (Doroshenko and Neher, 1992). A small conductance Cl^- channel (~4 pS) activated by cell swelling has also been observed in epithelial cells (Kunzelmann, Kubitz, Grolik, Wart, and Greger, 1992) and Jurkat cells (Lewis et al., 1993). The high conductance Cl^--channels described in endothelial cells (Groschner and Kukovetz, 1992; Olesen and Bundgaard, 1992; Vaca and Kunze, 1993) are certainly not involved in the activation of the HTS-induced current.

GTPγS activated a current that is similar to the HTS-induced current in endothe-

lial cells, suggesting that a G-protein dependent mechanism may be involved in the activation of this current (see also Suzuki, Kawahara, Ogawa, Morita, Kawaguchi, Kurihara, and Sakai, 1990). A G-protein-mediated activation of phospholipase C is however rather unlikely. Neomycin binds to PIP_2 and makes this substrate unavailable for PLC (Reid and Gajjar, 1987). This should block activation of the HTS-induced current, but in none of the experiments did neomycin affect the HTS-induced current. This finding excludes a major contribution of the PLC pathway to the activation of the volume-induced Cl^- currents in endothelial cells.

Another target for a G-protein-mediated action could be PLA_2. Volume-activated chloride channels in chromaffin cells (Doroshenko, 1991) and epithelial cells (Kubo and Okada, 1992) are sensitive to the arachidonic acid metabolism. In heart muscle cells, arachidonic acid directly activates mechano-sensitive K^+-channels (Kim, 1992). In our experiments on endothelial cells we were not able to observe consistent effects of exogeneously added AA on ionic currents. However, both HTS and AA consistently released calcium from internal stores in these cells (unpublished observation). NDGA (lipoxygenase inhibitor) or indomethacin (cyclo-oxygenase inhibitor) did also not affect HTS-induced currents, so that we can exclude that products of the arachidonic acid metabolism are involved in the signal transduction of the volume changes. Activation of these currents was however completely abolished after block of PLA_2 with pBPB. Cleavage products of PLA_2 might therefore be involved in activation of the HTS-induced current, but not products downstream of arachidonic acid.

It has also been reported that cAMP induces configurational changes in endothelial cells which are coupled to activation of a Cl^--conductance (Ueda et al., 1990). Activation of the PKA pathway also activated high conductance (400 pS) Cl^-channels in pig (Groschner and Kukovetz, 1992) and bovine (Vaca and Kunze, 1993) aortic endothelial cells. The Cl^--channel activated by HTS in our experiments has however a much smaller conductance, and is not affected by PKI.

It has recently been shown that HTS-induced currents are associated with the human multi-drug-resistance P-glycoprotein (Gill et al., 1992; Valverde et al., 1992). Verapamil and a forskolin analog, DDFSK, that does not interfere with adenylate cyclase, blocked Cl^--currents that are related to P-glycoprotein (Valverde et al., 1992; Diaz et al., 1993). Our results in human endothelial cells support the hypothesis that the HTS-induced current may be related to ABC transporters. HTS-induced currents in endothelial cells show inactivation at positive potential. This inactivation is slower than that observed in fibroblasts (Valverde et al., 1992). These divergent results could be explained if we assume that the apparent inactivation is due to intracellular accumulation of Cl^- at positive potentials and a concomitant reduction of the Cl^- driving force, that occur at different rates in both cell types. P-glycoproteins can form a latent Cl^- channel (Gill et al., 1992), which becomes functional by binding of ATP. The amplitude of the HTS-induced current and its rate of activation are reduced during repetitive activation of cells which were perfused with ATP-free pipette solutions. This finding is compatible with a gradual ATP-depletion of the cells and a concomitant reduction of the P-glycoproteins in the ATP-bound form. This interpretation is supported by the accelerated decrease of the current if the rate of ATP-depletion is increased in the presence of inhibitors of the energy metabolism.

Furthermore, it has been shown that P-glycoproteins (encoded by the MDR1 gene) are functionally expressed in endothelial cells (Hegemann, Bauer, and Kerbel, 1992; our unpublished observations).

From all our data we conclude that changes in cell volume activate a Cl^- current in human endothelial cells via a G-protein mediated second messenger, which is not linked to PLC, PKC or PKA activation. Because of the many similarities with the P-glycoprotein-dependent volume activated Cl^- current we suppose a functional connection between HTS-induced currents and activation of a P-glycoprotein in human endothelial cells.

We are grateful to Dr. M. Bollen, KU Leuven (Belgium), Department of Biochemistry for his kind gift of PKA-inhibitor.

This work was supported by grants from the Max Planck Gesellschaft to B. Nilius, from the Onderzoeksfonds of the KU Leuven to M. Oike and I. Zahradnik.

Original version received 5 May 1993 and accepted version received 8 November 1993.

REFERENCES

Cantiello, H. F., A. G. Prat, J. V. Bonventre, C. C. Cunningham, J. H. Hartwig, and D. A. Ausiello. 1993. Actin-binding protein contributes to cell volume regulatory ion channel activation in melanoma cells. *Journal of Biological Chemistry.* 268:4596–4599.

Davies, P. F., and S. C. Tripathi. 1993. Mechanical stress mechanisms and the cell: an endothelial paradigm. *Circulation Research.* 72:239–245.

Diaz, M., M. A. Valverde, C. F. Higgins, C. Rucareanu, and F. V. Sepulveda. 1993. Volume-activated chloride channels in HeLa cells are blocked by verapamil and dideoxyforskolin. *Pflügers Archiv.* 422:347–353.

Doroshenko, P. 1991. Second messengers mediating activation of chloride current by intracellular GTPγS in bovine chromaffin cells. *Journal of Physiology.* 436:725–738.

Doroshenko, P., R. Penner, and E. Neher. 1991. A novel chloride conductance in the membrane of bovine chromaffin cells activated by intracellular GTPγS. *Journal of Physiology.* 436:711–724.

Doroshenko, P., and E. Neher. 1992. Volume-sensitive conductance in bovine chromaffin cell membrane. *Journal of Physiology.* 449:197–218.

Gill, D. R., S. C. Hyde, C. F. Higgins, M. A. Valverde, G. M. Minteng, and F. V. Sepulveda. 1992. Separation of drug transport and chloride channel functions of human multidrug resistance P-glycoprotein. *Cell.* 71:23–32.

Grinstein, S., and J. K. Foskett. 1990. Ionic mechanisms of cell volume regulation in leukocytes. *Annual Review of Physiology.* 52:399–414.

Groschner, K., and W. R. Kukovetz. 1992. Voltage-sensitive chloride channels of large conductance in the membrane of pig aortic endothelial cells. *Pflügers Archiv.* 421:209–217.

Grynkiewicz, G., M. Poenie, and R. Y. Tsien. 1985. A new generation of Ca^{2+} indicators with greatly improved fluorescence properties. *Journal of Biological Chemistry.* 260:3440–3450.

Hegemann, E. J., H. C. Bauer, and R. S. Kerbel. 1992. Expression and functional activity of P-glycoprotein in cultured cerebral capillary endothelial cells. *Cancer Research.* 52:6969–6975.

Hoffmann, E. K., and L. O. Simonson. 1989. Membrane mechanisms in volume and pH regulation in vertebrate cells. *Physiological Reviews.* 69:315–382.

Horn, R., and A. Marty. 1988. Muscarinic activation of ionic currents measured by a new whole-cell recording method. *Journal of General Physiology.* 92:145–159.

Jaffe, E. A., R. L. Nachman, C. G. Becker, and C. R. Minick. 1973. Culture of human endothelial cells derived from umbilical veins. *Journal of Clinical Investigation.* 52:2745–2756.

Kempski, O., M. Spatz, G. Valet, and A. Baethman. 1985. Cell volume regulation of cerebrovascular endothelium in vitro. *Journal of Cellular Physiology.* 123:51–54.

Kim, D. 1992. A mechanosensitive K^+ channel in heart cells: activation by arachidonic acid. *Journal of General Physiology.* 100:1021–1040.

Knighton, D. R., J. Zheng, L. F. Ten Eyck, N.-H. Xuong, S. S. Taylor, and J. M. Sowadski. 1991. Structure of a peptide inhibitor bound to the catalytic subunit of cyclic adenosine monophosphate-dependent protein kinase. *Science.* 253:414–420.

Knoblauch, C., M. H. Montrose, and H. Murere. 1989. Regulatory volume decrease by cultured renal cells. *American Journal of Physiology.* 256:C252–C259.

Korn, S. J., and R. Horn. 1989. Influence of sodium-calcium exchange on calcium current rundown and the duration of calcium-dependent chloride currents in pituitary cells, studied with whole cell and perforated patch recording. *Journal of General Physiology.* 94:789–812.

Kubo, M., and Y. Okada. 1992. Volume-regulatory Cl^- channel currents in cultured human epithelial cells. *Journal of Physiology.* 456:351–371.

Kunzelmann, K., R. Kubitz, M. Grolik, R. Wart, and R. Greger. 1992. Small-conductance Cl^- channels in HT_{29} cells: activation by Ca^{2+}, hypotonic cell swelling and 8-Br-cGMP. *Pflügers Archiv.* 421:238–246.

Ling, B. N., and W. C. O'Neill. 1992. Ca^{2+}-dependent and Ca^{2+}-permeable ion channels in aortic endothelial cells. *American Journal of Physiology.* 263:H1827–H1838.

Lewis, R. S., P. E. Ross, and M. D. Cahalan. 1993. Chloride channels activated by osmotic stress in T lymphocytes. *Journal of General Physiology.* 101:801–826.

McCarty, N. A., and R. G. O'Neill. 1992. Calcium signalling in cell volume regulation. *Physiological Reviews.* 72:1037–1061.

Morris, C. E. 1990. Mechanosensitive ion channels. *Journal of Membrane Biology.* 113:93–107.

Neher, E. 1989. Combined Fura-2 and patch clamp measurements in rat peritoneal mast cells. *In* Neuromuscular Junction. L. C. Sellin, R. Libelius, S. Thesleff, editors. Elsevier Science Publishers, Amsterdam. 65–76.

Nilius, B. 1993. Ion channels in non-excitable cells. *In* Principles of Cell Physiology and Biophysics. N. Sperelakis, editor. Academic Press, New York. In press.

Olesen, S. P., and M. Bundgaard. 1992. Chloride-selective channels of large conductance in bovine aortic endothelial cells. *Acta Physiologica Scandinavia.* 144:191–198.

O'Neill, W. C., and J. D. Klein. 1992. Regulation of vascular endothelium cell volume by Na^+-K^+-Cl^--cotransport. *American Journal of Physiology.* 62:C436–C444.

Sackin, H. 1989. A stretch-activated K^+ channel sensitive to cell volume. *Proceedings of the National Academy of Sciences, USA.* 86:1731–1735.

Schwarz, G., G. Callewaert, G. Droogmans, and B. Nilius. 1992. Shear stress-induced calcium transients in endothelial cells from human umbilical cord veins. *Journal of Physiology.* 458:527–538.

Sigworth, F. J. 1980. The variance of sodium current fluctuations at the node of Ranvier. *Journal of Physiology.* 307:97–129.

Suzuki, M., K. Kawahara, A. Ogawa, T. Morita, Y. Kawaguchi, S. Kurihara, and O. Sakai. 1990. $[Ca^{2+}]_i$ rises via G protein during regulatory volume decrease in rabbit proximal tubule cells. *American Journal of Physiology.* 258:F690–F6996.

Ueda, S., S.-L. Lee, and B. L. Fanburg. 1990. Chloride efflux in cyclic AMP-induced configurational changes of bovine pulmonary artery endothelial cells. *Circulation Research.* 66:957–967.

Vaca, L., and D. L. Kunze. 1993. cAMP-dependent phosphorylation modulates voltage gating in an endothelial Cl^--channel. *American Journal of Physiology.* 264:C370–C375.

Valverde, M. A., M. Diaz, M. Sepulveda, D. G. Gill, S. C. Hyde, and C. F. Higgins. 1992. Volume-regulated chloride channels are associated with the human multidrug-resistance P-glycoprotein. *Nature.* 355:830–833.